

4

AD-A213 167

CHEMICAL
RESEARCH,
DEVELOPMENT &
ENGINEERING
CENTER

CRDEC-CR-040

CLEARING OF MILITARY SMOKES AND AEROSOLS

Greg Hogan

GEO-CENTERS, INC.
Newton Centre, MA 02159

Glenn O. Rubel, Ph.D.
RESEARCH DIRECTORATE

August 1939

DTIC
ELECTE
OCT 03 1989
S E D

DISTRIBUTION STATEMENT A

Approved for public release;
Distribution Unlimited

U.S. ARMY
ARMAMENT
MUNITIONS
CHEMICAL COMMAND



Aberdeen Proving Ground, Maryland 21010-5423

89 10 3 113

Disclaimer

The findings in this report are not to be construed as an official Department of the Army position unless so designated by other authorizing documents.

Distribution Statement

Approved for public release; distribution is unlimited.

REPORT DOCUMENTATION PAGE				Form Approved OMB No. 0704-0188	
1a. REPORT SECURITY CLASSIFICATION UNCLASSIFIED			1b. RESTRICTIVE MARKINGS		
2a. SECURITY CLASSIFICATION AUTHORITY			3. DISTRIBUTION / AVAILABILITY OF REPORT Approved for public release; distribution is unlimited.		
2b. DECLASSIFICATION / DOWNGRADING SCHEDULE					
4. PERFORMING ORGANIZATION REPORT NUMBER(S) CRDEC-CR-040			5. MONITORING ORGANIZATION REPORT NUMBER(S)		
6a. NAME OF PERFORMING ORGANIZATION see reverse		6b. OFFICE SYMBOL (If applicable)	7a. NAME OF MONITORING ORGANIZATION		
6c. ADDRESS (City, State, and ZIP Code)			7b. ADDRESS (City, State, and ZIP Code)		
8a. NAME OF FUNDING / SPONSORING ORGANIZATION CRDEC		8b. OFFICE SYMBOL (If applicable) SMCCR-RSP-B	9. PROCUREMENT INSTRUMENT IDENTIFICATION NUMBER DAAA15-88-C-0050		
8c. ADDRESS (City, State, and ZIP Code) Aberdeen Proving Ground, MD 21010-5423			10. SOURCE OF FUNDING NUMBERS		WORK UNIT ACCESSION NO.
			PROGRAM ELEMENT NO.		
11. TITLE (Include Security Classification) Clearing of Military Smokes and Aerosols					
12. PERSONAL AUTHOR(S) Hogan, Greg (Geo-Centers, Inc.), and Rubel, Glenn O., Ph.D. (CRDEC)					
13a. TYPE OF REPORT Contractor		13b. TIME COVERED FROM 88 Aug To 89 Feb		14. DATE OF REPORT (Year, Month, Day) 1989 August	
15. PAGE COUNT 42					
16. SUPPLEMENTARY NOTATION COR: Dr. G. Rubel, SMCCR-RSP-B, (301) 671-2395					
17. COSATI CODES			18. SUBJECT TERMS (Continue on reverse if necessary and identify by block number)		
FIELD	GROUP	SUB-GROUP	Smoke scavenging Particle charge distribution conductors Triboelectrification (continued on reverse)		
07	04				
19. ABSTRACT (Continue on reverse if necessary and identify by block number) A new device has been developed to measure the charge distribution of candidate smoke scavenger materials that are advertently charged with corona fields and by triboelectrification. It was shown that particle saturation charge can be achieved with triboelectrification and that conductors charged more easily than dielectrics. It is also shown that particle shape has an influence on maximum particle charge. A phase II study is proposed that will attempt to extend the particle charge measurements to millimeter-sized scavenger particles.					
20. DISTRIBUTION / AVAILABILITY OF ABSTRACT <input checked="" type="checkbox"/> UNCLASSIFIED/UNLIMITED <input type="checkbox"/> SAME AS RPT. <input type="checkbox"/> DTIC USERS			21. ABSTRACT SECURITY CLASSIFICATION UNCLASSIFIED		
22a. NAME OF RESPONSIBLE INDIVIDUAL SANDRA J. JOHNSON			22b. TELEPHONE (Include Area Code) (301) 671-2914		22c. OFFICE SYMBOL SMCCR-SPS-T

UNCLASSIFIED

6. NAME OF PERFORMING ORGANIZATION

Geo-Centers, Inc.
7 Wells Avenue
Newton Centre, MA 02159

CRDEC
SMCCR-RSB-B
Aberdeen Proving Ground, MD 21010-5423

18. SUBJECT TERMS (continued)

Dielectrics,
Corona,

PREFACE

The work described in this report was authorized under Contract No. DAAA15-88-C-0050. This work was started in August 1988 and completed in February 1989.

The use of trade names or manufacturers' names in this report does not constitute an official endorsement of any commercial products. This report may not be cited for purposes of advertisement.

Reproduction of this document in whole or in part is prohibited except with permission of the Commander, U.S. Army Chemical Research, Development and Engineering Center, ATTN: SMCCR-SPS-T, Aberdeen Proving Ground, Maryland 21010-5423. However, the Defense Technical Information Center and the National Technical Information Service are authorized to reproduce the document for U.S. Government purposes.

This report has been approved for release to the public.



Accession For	
NTIS GRA&I	<input checked="checked" type="checkbox"/>
DTIC TAB	<input type="checkbox"/>
Unannounced	<input type="checkbox"/>
Justification	
By	
Distribution/	
Availability Codes	
Dist	Avail and/or Special
A-1	

Blank

CONTENTS

	Page
1. INTRODUCTION	9
2. THEORY OF SCAVENGER CHARGE MEASUREMENT	11
3. THEORY OF SCAVENGER PARTICLE CHARGING	13
4. EXPERIMENTAL METHOD AND RESULTS	18
4.1 Description of the Experimental Setup	18
4.2 Particle Charge Distribution Experiments ...	19
4.3 Active Corona Discharge Particle Charging ..	35
4.4 Triboelectric Particle Charging	39
4.5 Terminal Velocity Experiments	39
5. CONCLUSIONS AND RECOMMENDATIONS	41
REFERENCES	42

LIST OF FIGURES AND TABLE

Figures

1.	Schematic of Particle and Forces in Electrostatic Balance	12
2.	Schematic of Phase I Apparatus for Entraining, Changing and Measuring Charge of Candidate Scavenger Particles	14
3.	Distortion of Electric Field Around Uncharged Particle	16
4.	Distortion of Electric Field Around Partially Charged Particle	16
5.	Charge Distribution for Aluminum (particle size 22μ). The Corona Discharge was Off and the Initial Electrostatic Balance Plate Voltage was 25 volts	21
6.	Charge Distribution for Aluminum (particle size 22μ). The Corona Discharge was Off and the Initial Electrostatic Balance Plate Voltage was 50 Volts	22
7.	Charge Distribution for Aluminum. Corona Discharge Device was Off. The Initial Electrostatic Balance Plate Voltage was 100 Volts	23
8.	Charge Distribution for Aluminum (particle size 22μ). The Corona Discharge was Off and the Initial Electrostatic Balance Plate Voltage was 150 Volts	24
9.	Charge Distribution for Aluminum (particle size 22μ). The Corona Discharge was Off and the Initial Electrostatic Balance Plate Voltage was 200 Volts	25
10.	Charge Distribution for Aluminum (particle size 22μ). The Corona Discharge was Off and the Initial Electrostatic Balance Plate Voltage was 400 Volts	26
11.	Charge Distribution for Aluminum. Corona Discharge Device was Off. The Initial Electrostatic Balance Plate Voltage was 100 Volts	27

12.	Charge Distribution for Copper. Corona Discharge Device was Off. The Initial Electrostatic Balance Plate Voltage was 100 Volts	28
13.	Charge Distribution for Iron. Corona Discharge Device was Off. The Initial Electrostatic Balance Plate Voltage was 100 Volts	29
14.	Charge Distribution for Lead. Corona Discharge Device was Off. The Initial Electrostatic Balance Plate Voltage was 100 Volts	30
15.	Charge Distribution for Magnesium. Corona Discharge Device was Off. The Initial Electrostatic Balance Plate Voltage was 100 Volts	31
16.	Charge Distribution for Glass Micro-Sphere. Corona Discharge Device was Off. The Initial Electrostatic Balance Plate Voltage was 100 Volts	32
17.	Charge Distribution for Graphite. Corona Discharge Device was Off. The Initial Electrostatic Balance Plate Voltage was 100 Volts	33
18.	Charge Distribution for Aluminum (particle size 22μ). The Corona Discharge was Active and the Initial Electrostatic Balance Plate was 100 Volts	36
19.	Charge Distribution for Copper (particle size 46μ). The Corona Discharge was Active and the Initial Electrostatic Balance Plate was 100 Volts	37
20.	Charge Distribution for Glass (particle size 22μ). The Corona Discharge was Active and the Initial Electrostatic Balance Plate was 100 Volts	38
21.	Effect of Charging Method on Particle Charge (Aluminum, 22μ). Initial Plate Voltage: 100 Volts	40

TABLE

1.	Maximum Observed and Theoretical Particle Charge For Al, Cu, Fe, Pb, Mg, Graphite and Glass, as Calculated From Equations 1 and 7 and Figures 11-17	34
----	--	----

CLEARING OF MILITARY SMOKES AND AEROSOLS

1. INTRODUCTION

The clearing of military smokes and aerosols to improve visibility in a battlefield situation, whether it be large area clearing or line of sight, is of great interest and decidedly important for tactical and reconnaissance purposes. One of the most effective methods to remove smoke and aerosol particles is a technique known as Smoke Particle Deposition on Scavengers (SPADES). SPADES is a technique to remove smoke particles by employing scavengers which drop through the obscuring cloud and deposit rapidly to the ground. The primary mechanism for the removal of particles is by inertial impaction enhanced by electrostatic attraction.

The removal efficiency of the clearing material can be greatly enhanced by increasing the charge on the scavenging material. The development and deployment of a charged scavenger smoke and aerosol clearing system requires the determination of scavenger total charge, and an evaluation of its ability to acquire and retain charge. Under this Phase I SBIR effort, GEO-CENTERS, INC. has determined the characteristic charge for a number of potential scavenger materials and has identified a low cost particle charging method.

The technical objectives as stated in the Phase I proposal were:

1. Literature Search - A literature search will be performed to identify additional, feasible candidate scavengers and identify techniques/methods for charging particles that are appropriate for obscuration clearing.

2. Experiments - The experimental portion is subdivided into three sub-tasks:

- a. Set-up of the characteristic charge/terminal velocity experimental apparatus and calibrate with aluminum scavenging particles. The aluminum scavengers are selected as a reference to adjust the corona discharge parameters (electrode gap and potential) and electrostatic balance potentials.
- b. Identification of appropriate scavenging materials and determination of their charge density.
- c. Determination of net charge and terminal velocity on scavenger materials as a function of particle size.

In this Phase I program, all of the technical objectives have been met. GEO-CENTERS, INC. has evaluated characteristic charge distributions for a number of potential scavenger materials including conductors (aluminum, copper, lead, iron, graphite) and a dielectric (glass), and found the conductors of the same size to have up to 5-10 times higher characteristic particle charge than the dielectric. In addition, a significant increase in conductor charging (aluminum) was produced by passing the scavenging material through a ten foot length of plastic tubing. This triboelectric charging mechanism represents a potentially simple, rugged, low cost and low power method for both charging scavenger material and introducing the material into the environment for smoke and aerosol clearance.

This technical report is divided into four subsections: Theory of Scavenger Charge Measurement, Theory of Scavenger Particle Charging, Experimental Method and Results, and Conclusions and Recommendations.

The first two subsections describe the theoretical basis for determining the charge resident on observed scavenger particles and an active, corona discharge method of charging those scavenger particles. Experimental Method and Results includes a presentation of the characteristic charge distributions for selected scavenger materials and a comparison of these values with the theoretical values. In addition, experimental results for the corona discharge device are presented for each scavenger particle tested. Finally, the triboelectric charging and terminal velocity results are presented and discussed. Conclusions drawn from this research effort and recommendations for Phase II research and development are presented in the last section.

2. THEORY OF SCAVENGER CHARGE MEASUREMENT

The theory for determining observed scavenger particle charge is based on the original apparatus developed by Robert Millikan to measure charge on oil droplets. In this apparatus, the charged particle in question is electrostatically balanced between two conducting plates with an applied potential. When the particle is suspended between the plates with net zero velocity, the gravitational downward force is balanced by the upward electrostatic force as shown in Figure 1. The balancing equation is:

$$Eq = mg$$

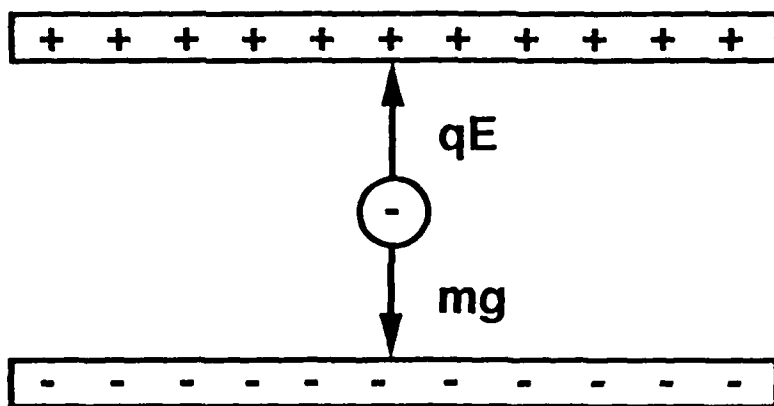


Figure 1. Schematic of Particle and Forces
in Electrostatic Balance

where E is the electric field between the plates and can be written as V/h where V is the applied plate voltage and h is the plate separation. The particle charge is q and m is its mass which is calculated knowing material density, ρ , and volume. Assuming that scavenger particles are approximately spherical, the volume is simply equal to $4/3 \pi (d/2)^3$ where d is particle diameter. Once a scavenger particle is balanced with an applied voltage, V, its charge is :

$$q = \frac{\rho \cdot \text{vol} \cdot g \cdot h}{V} \quad (1)$$

3. THEORY OF SCAVENGER PARTICLE CHARGING

Utilization of electrical force is considered the most feasible mechanism for effective smoke and aerosol removal by scavengers¹. Increasing the charge on the scavenging material greatly enhances its scavenging efficiency. GEO-CENTERS, INC. has examined two particle charging methods: an active mechanism, corona discharge, and a passive mechanism, triboelectric charging.

The corona discharge device and particle entrainment arrangement is depicted in Figure 2. A constant discharge potential is maintained between the anode needle and the cathode plate. The scavenger particles are charged as they pass through the corona field, E_c .

For a given corona field strength, the saturation charge represents the maximum charge a particle can attain for that field strength. Using the derivation of Reist², the saturation charge is determined below.

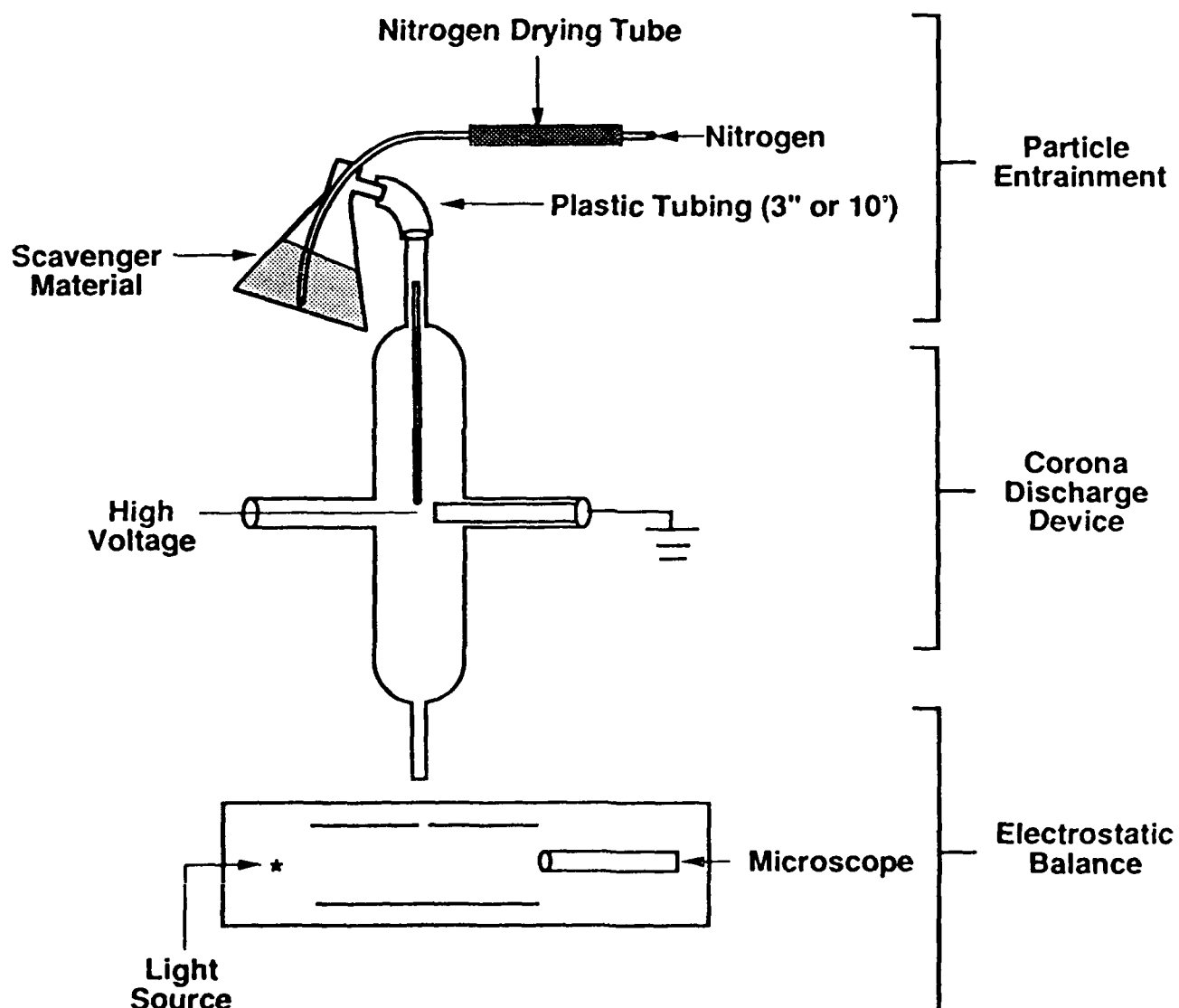


Figure 2. Schematic of Phase I Apparatus for Entraining, Changing and Measuring Charge of Candidate Scavenger Particles

The normal component of the electric field, E , at any point on the surface of a spherical particle placed in an initially uniform electric field is:

$$E_1 = pE_C \cos\theta \quad (2)$$

where $p = 3\epsilon/(\epsilon+2)$ and ϵ is the dielectric constant of the sphere. The value of p will generally be between 1.5 and 2 for dielectric particles and will be 3 for conducting particles ($\epsilon = \infty$). The initially uniform field near the particle will be distorted as shown in Figure 3. The corona-generated ions follow the field lines that intercept the particle surface, thereby charging the particle. The accumulation of charge on the sphere creates a secondary electric field which acts to retard the accumulation of additional charge. The repelling field E_2 is derived by Gauss' law and is given by

$$E_2 = \frac{-4q}{d^2 4\pi\epsilon_0} \quad (3)$$

The presence of E_2 alters the field pattern and consequently reduces the charging rate. Figure 4 shows the field configuration when half the saturation charge on the particle is reached. Note that the electric flux, $\psi(q)$, defined as $\oint E \cdot ds$, has changed.

The total electric flux entering the particle is:

$$\psi(q) = 2 \int_0^{\theta_0} \left(pE_C \cos\theta - \frac{4q}{d^2 4\pi\epsilon_0} \right) \left(\frac{\pi}{2} \right) d^2 \sin\theta d\theta \quad (4)$$

which on integration becomes:

$$\psi(q) = p \frac{\pi d^2}{4} E_C \left(1 - \frac{q}{pE_C \pi \epsilon_0 d^2} \right)^2 \quad (5)$$

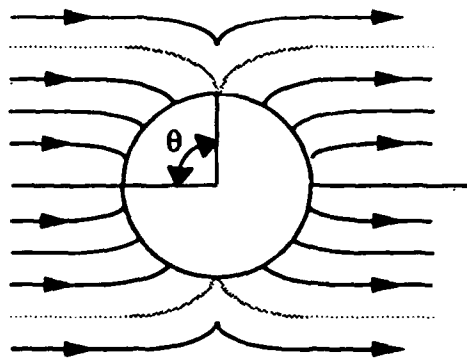


Figure 3. Distortion of Electric Field Around an Uncharged Particle

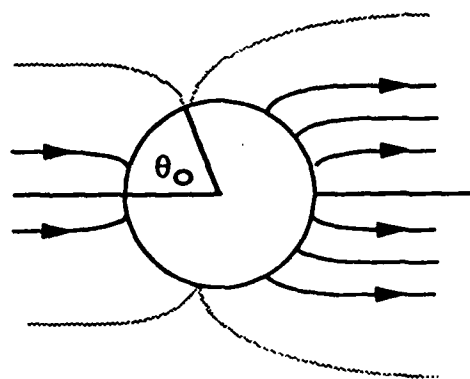


Figure 4. Distortion of Electric Field Around a Partially Charged Particle

The limiting or saturation charge (q_s) occurs when $\psi(q) = 0$. Replacing q with q_s and solving equation 5 for q_s gives

$$q_s = pE_C d^2 \pi \epsilon_0 \quad (6)$$

The maximum field generated before breakdown of the air by the corona device is approximately 10 kv/cm which corresponds to a particle saturation charge of

$$q_s = pd^2 (2.8 \times 10^{-5}) \text{ coulombs} \quad (7)$$

It should be noted that the value of 10 kv/m is the maximum electric field that can be supported in air by any field generating method, not just the corona discharge apparatus. Therefore, equation 7 represents the saturation charge, based on a Gaussian surface argument, that a particle can attain in air regardless of the charging mechanism. Particle charge saturation is not an instantaneous event. It has been shown that the charge, q , acquired after t seconds is

$$q = q_s \frac{t}{t + \tau} \quad (8)$$

The particle charging time constant, τ , is the time required to reach half the saturation charge. The particle attains 91% of its limiting or saturation value in 10τ seconds.

4. EXPERIMENTAL METHOD AND RESULTS

4.1 Description of the Experimental Setup

A schematic of the experimental apparatus for measuring particle charge is shown in Figure 2. The experiment can be divided into three separate steps: particle entrainment, particle charging, and measurement of the particle charge.

The particles are transported through the apparatus by entrainment in a nitrogen flow. The nitrogen carrier gas is first passed through a drying tube (Supelco, INC.) and the flow is then directed into a container which holds the sample particles. The inflow of the nitrogen provides sufficient agitation to entrain the particles in the outflow. The entrainment of the particles is further facilitated by periodic manual agitation of the chamber containing the particles.

Both active and passive methods are employed to charge the particles in this experiment. Active charging of the particles involves the introduction of the particles into a field of free electrons produced by an active corona inside the discharge device. The corona is produced by increasing the potential difference between a point-anode and a grounded plate (held at a fixed separation of approximately 1cm) until electrical breakdown of the gas occurs. The breakdown of the gas in this region and the resulting cascade of electrons to the plate produces a corona, which is characterized by a blue glow in the gap between the point and plate. With a gap of approximately 1cm, a corona is achieved with an applied voltage of approximately 10 kV. Care is taken not to exceed this voltage which would result in a catastrophic breakdown of the gas and corresponding spontaneous discharge across the gap, which would carbonize the plate and interfere with subsequent corona generation.

Passive charging of the particles is accomplished by passing the entrained particles through 10 feet of plastic tubing with the corona field off. The actual charging mechanism is believed to be triboelectrification, but this has not been confirmed.

An electrostatic balance (Central Scientific) is used to measure the charge resident on the particles after either passive or active charging of the particles. The electrostatic balance consists of an insulated chamber with conducting plates on the top and bottom which are charged with opposite polarity. A microscope and a high intensity light source are inserted through ports in the wall of the chamber to facilitate observation of the particles. A potential across the balancing plates is produced by either a Kepco Power Supply, which is used when large voltages (up to 1,000V) are required, or a Leader Power Supply, which is used when voltages of less than 100 volts are needed. The voltage across the plates is monitored by a Fluke digital multimeter. Following the principles of electrostatic balancing outlined in the Theory Section (2.0), a selected initial voltage is applied across the plates just after a particle enters the balance through a hole in the top plate. The initial voltage is adjusted until the selected particle is balanced between the plates. The final voltage across the plates is recorded as the balancing voltage for the particle.

4.2 Particle Charge Distribution Experiments

Experiments were performed to determine the characteristic charge of potential scavenger materials. A number of materials were considered, including conductors (Al, Cu, Fe, Pb, Mg and graphite), dielectrics (glass, poly-mag 80), and carbon fibers and chaff (aluminized mylar). All materials were characterized except

for the chaff which we were unable to procure in time, and the poly-mag 80. The poly-mag 80 was supplied as a filter consisting of stiff fibers several inches in length. Efforts to reduce the fiber size to 10's of microns for evaluation in our apparatus were unsuccessful.

Each material is sieved to produce a discrete range of particle sizes (20-25 and 45-47 μm) and the characteristic charge distribution is experimentally determined initially with the corona device inactive (not passive, 10' tubing experiment). Figures 5-10 show characteristic charge distributions for aluminum over a range of initial plate voltages, 25, 50, 100, 150, 200 and 400 volts. This suite of initial voltage settings illustrates the dependency of the mean charge distribution on the initial setting. The broad range in particle charge for aluminum is also observed for the other materials tested. Plate voltage and particle charge are inversely proportional. Therefore, measurement of the charge distribution for more highly charged particles is performed with an initial value of 100 volts. This initial voltage setting is chosen to ensure the capture of higher momentum particles.

Figures 11-17 show characteristic charge distributions for Al, Cu, Fe, Pb, Mg, Glass and Graphite. Individual particle electrical charge can be calculated using Equation 1. The maximum particle charge and the mean charge of the distributions are listed in Table 1. Also, the theoretical maximum charge for each particle that could be obtained via a corona device in air is reported. Finally, the ratio of observed charge to maximum theoretical charge is calculated.

Text continues on page 35.

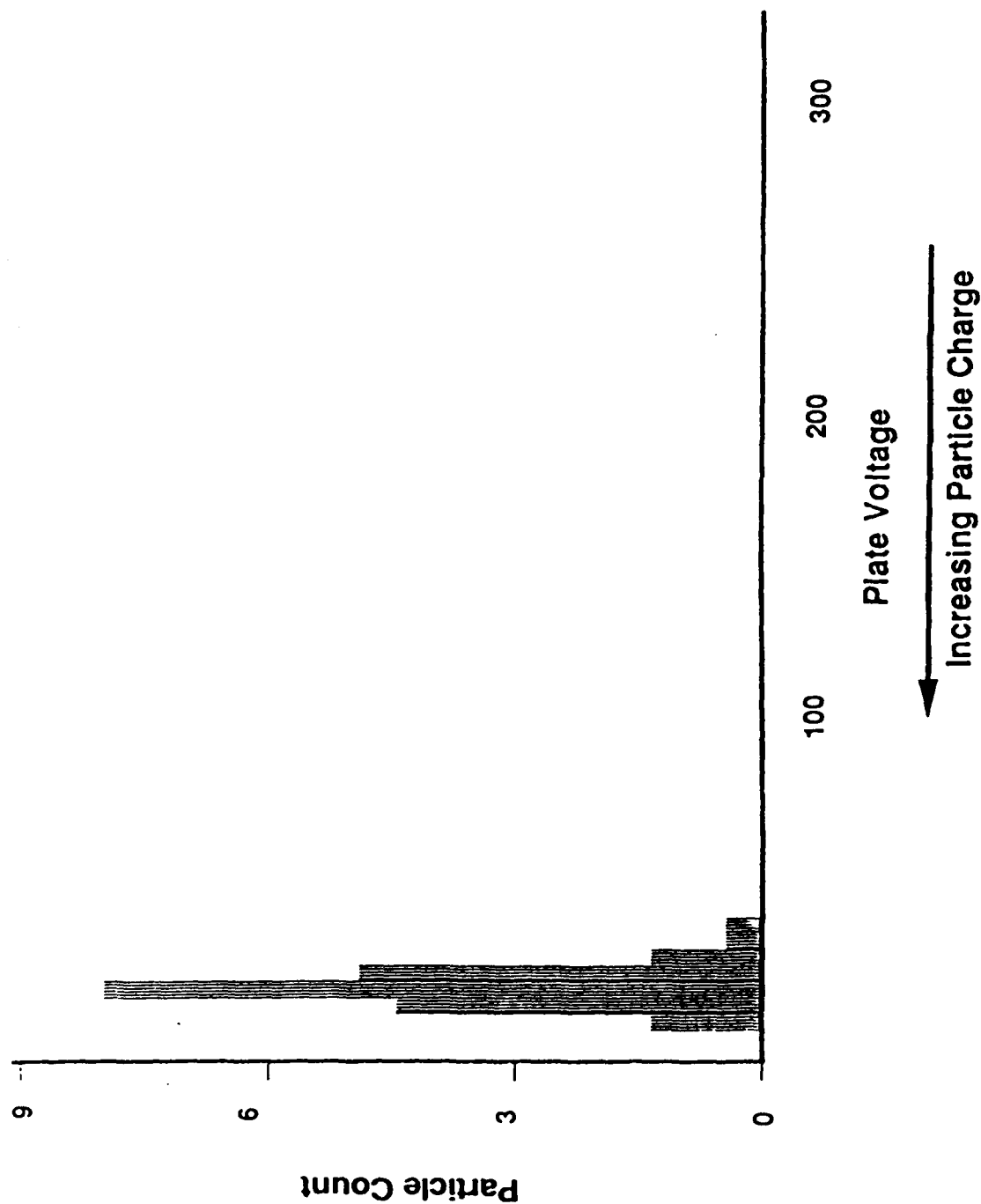


Figure 5
Charge Distribution For Aluminum (particle size 22μ). The Corona Discharge Was Off And The Initial Electrostatic Balance Plate Voltage Was 25 Volts.

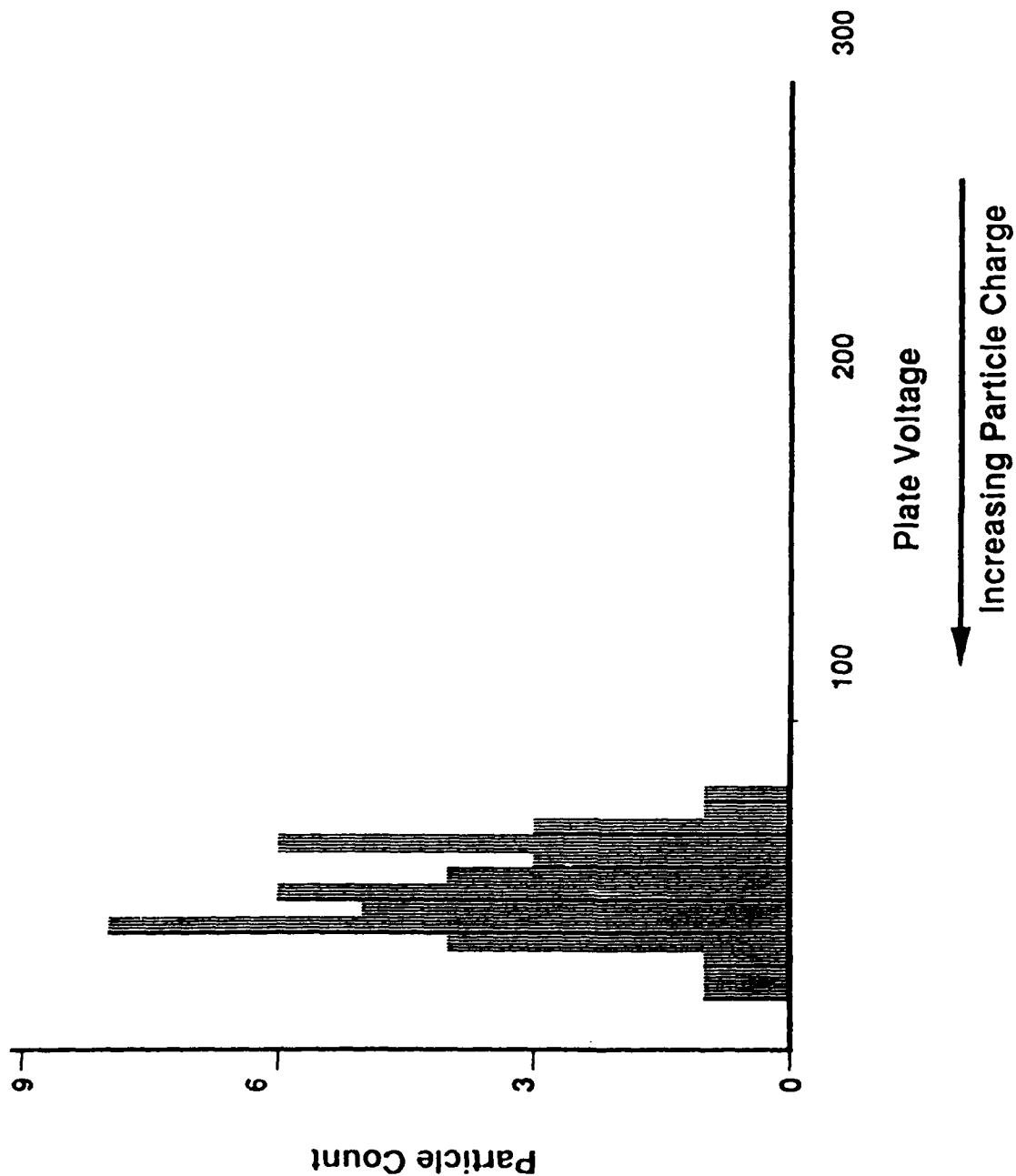


Figure 6
 Charge Distribution For Aluminum (particle size 22 μ). The Corona Discharge Was Off And The Initial Electrostatic Balance Plate Voltage Was 50 Volts.

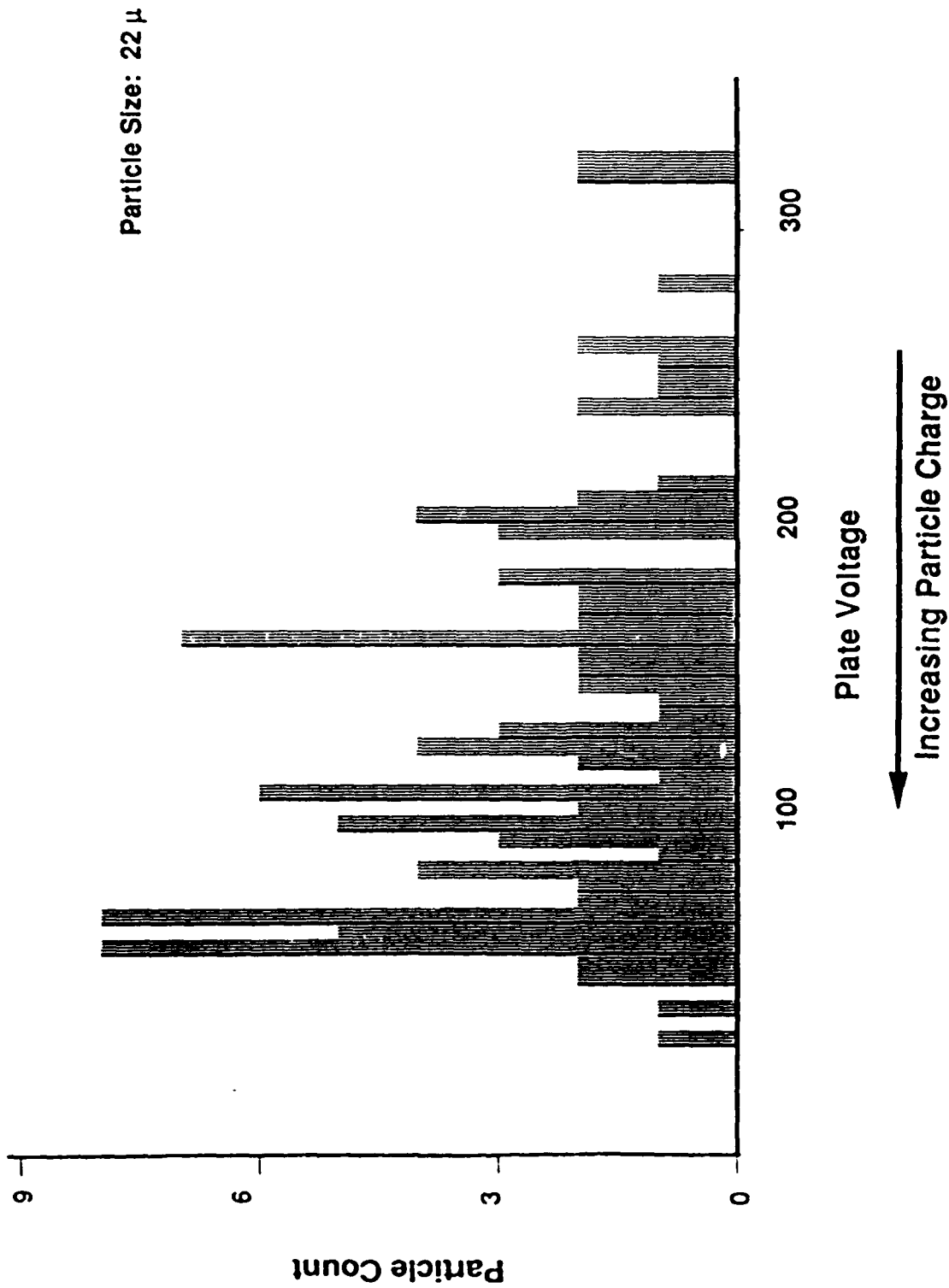


Figure 7

Charge Distribution for Aluminum. Corona Discharge Device was Off. The Initial Electrostatic Balance Plate Voltage was 100 Volts.

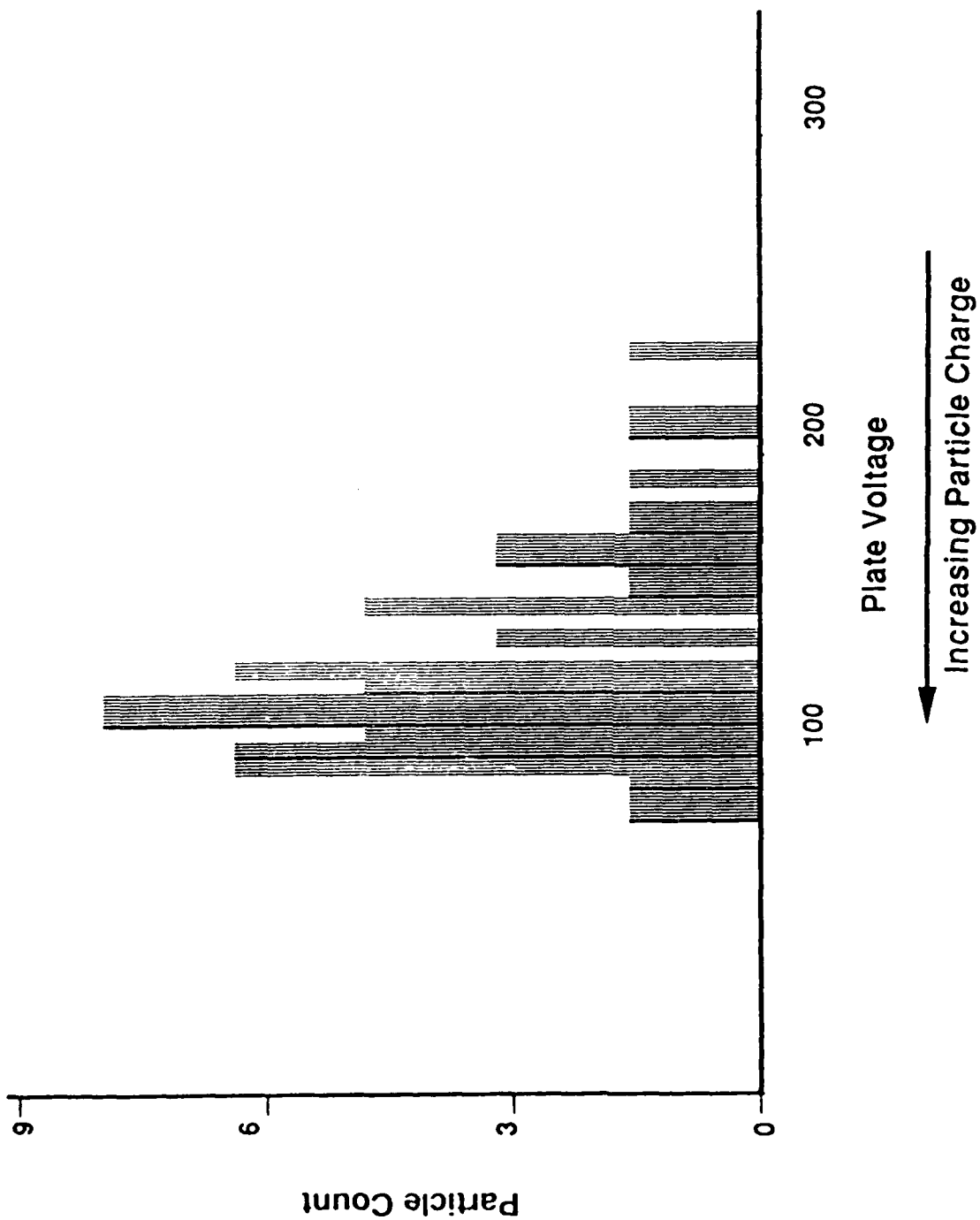


Figure 8
Charge Distribution For Aluminum (particle size 22μ). The Corona Discharge Was Off And The Initial Electrostatic Balance Plate Voltage Was 150 Volts.

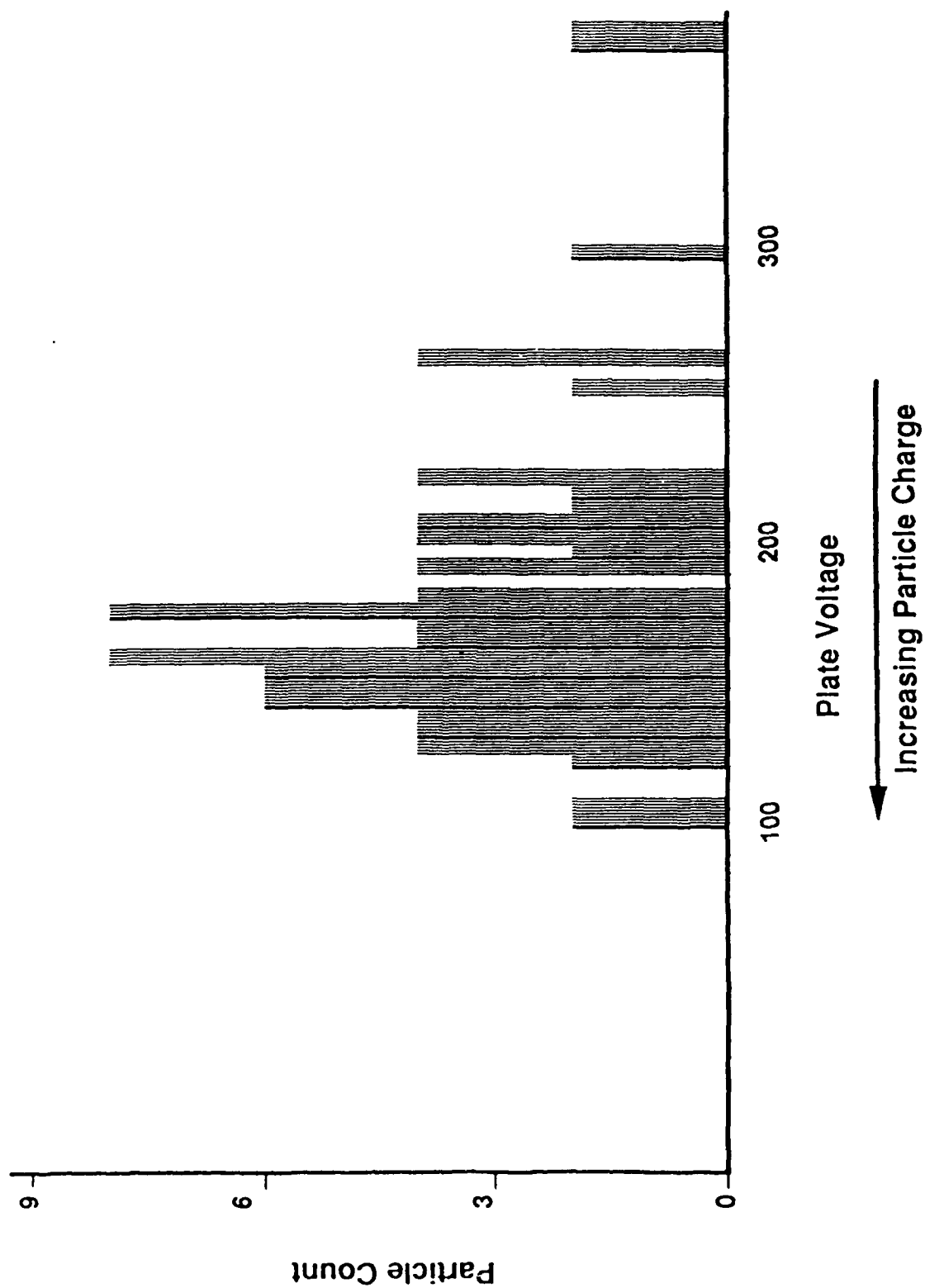


Figure 9
Charge Distribution For Aluminum (particle size 22μ). The Corona Discharge Was Off And The Initial Electrostatic Balance Plate Voltage Was 200 Volts.

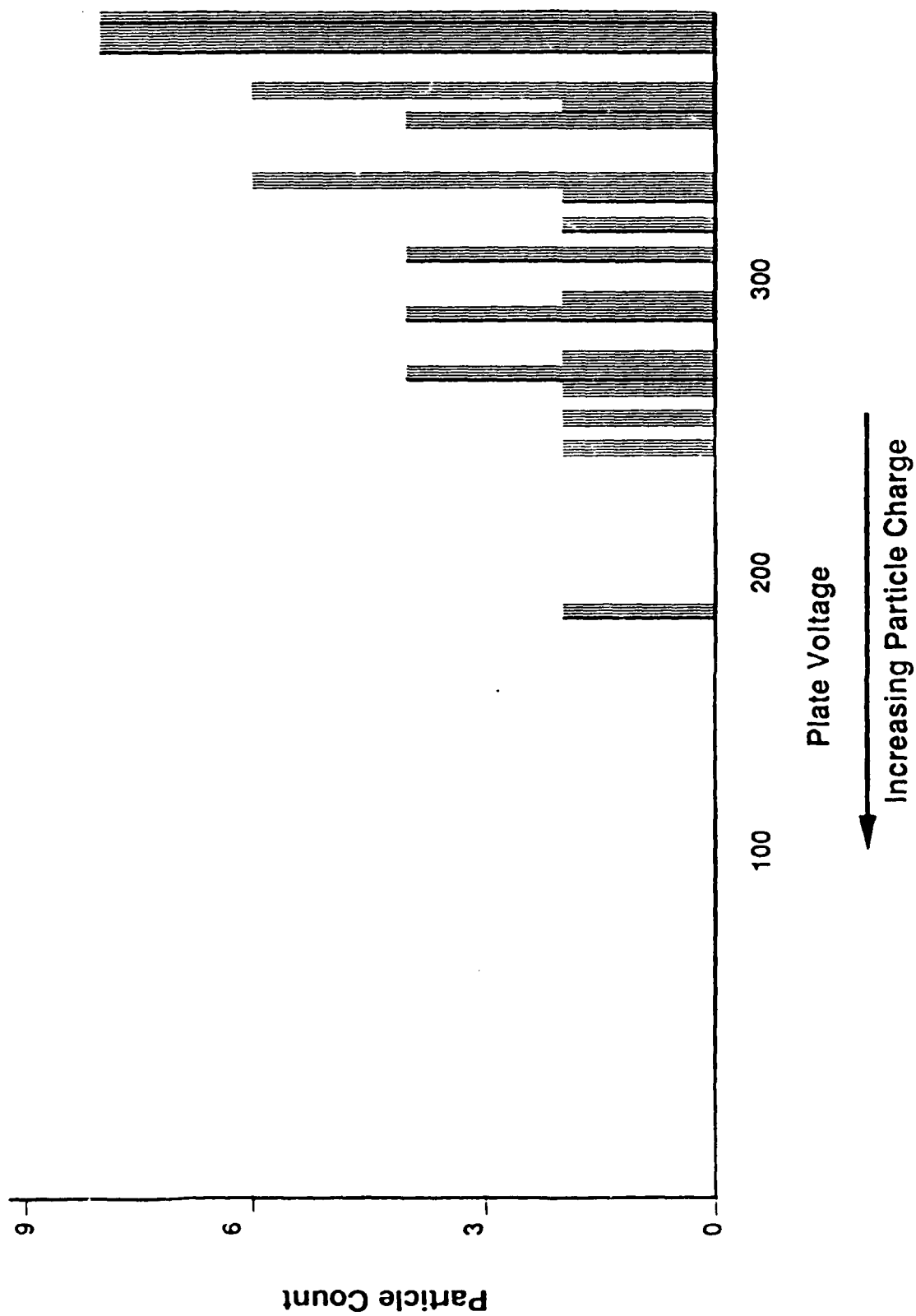


Figure 10
 Charge Distribution For Aluminum (particle size 22μ). The Corona Discharge Was Off And The Initial Electrostatic Balance Plate Voltage Was 400 Volts.

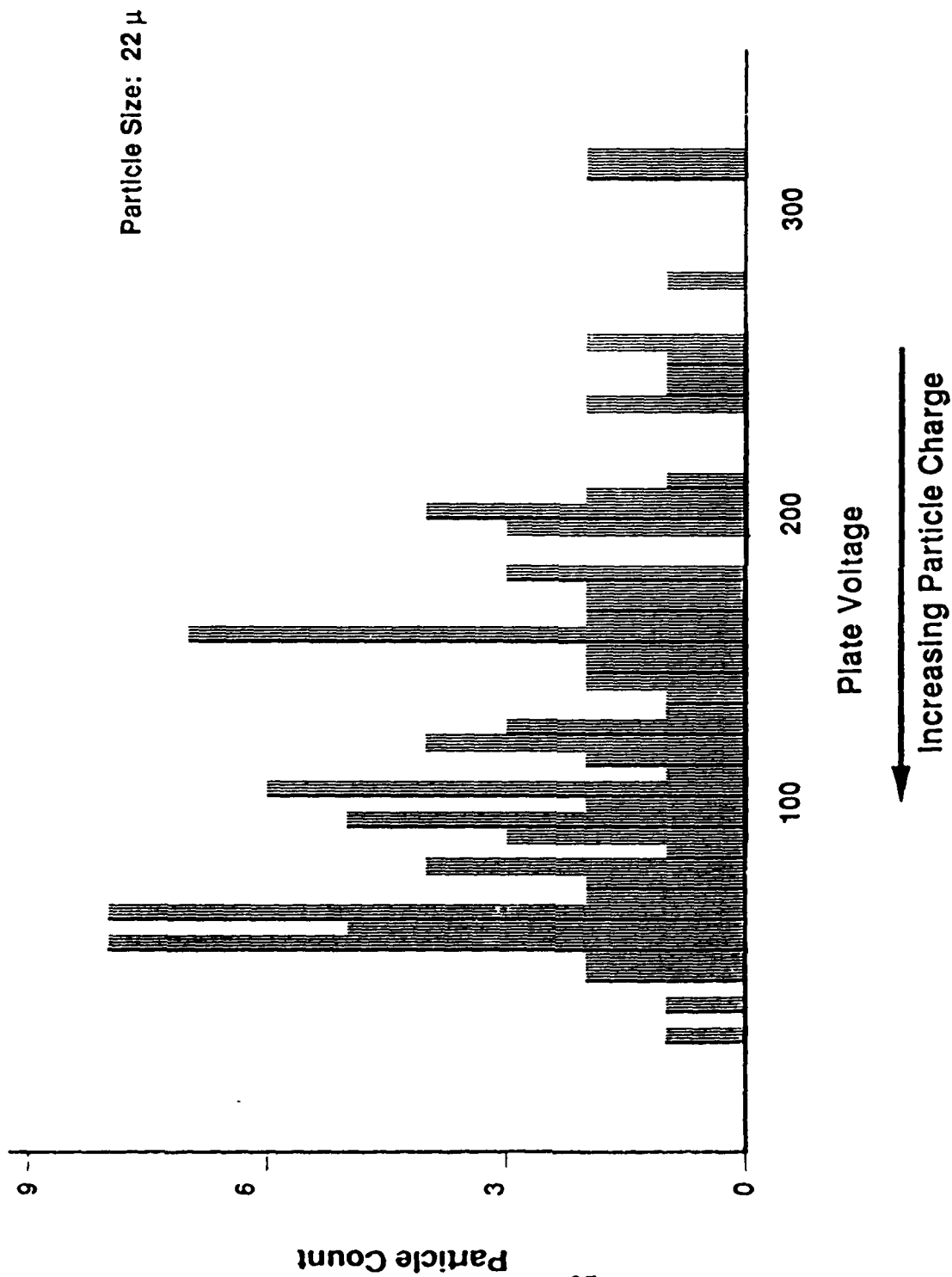


Figure 1 1

Charge Distribution for Aluminum. Corona Discharge Device was Off. The Initial Electrostatic Balance Plate Voltage was 100 Volts.

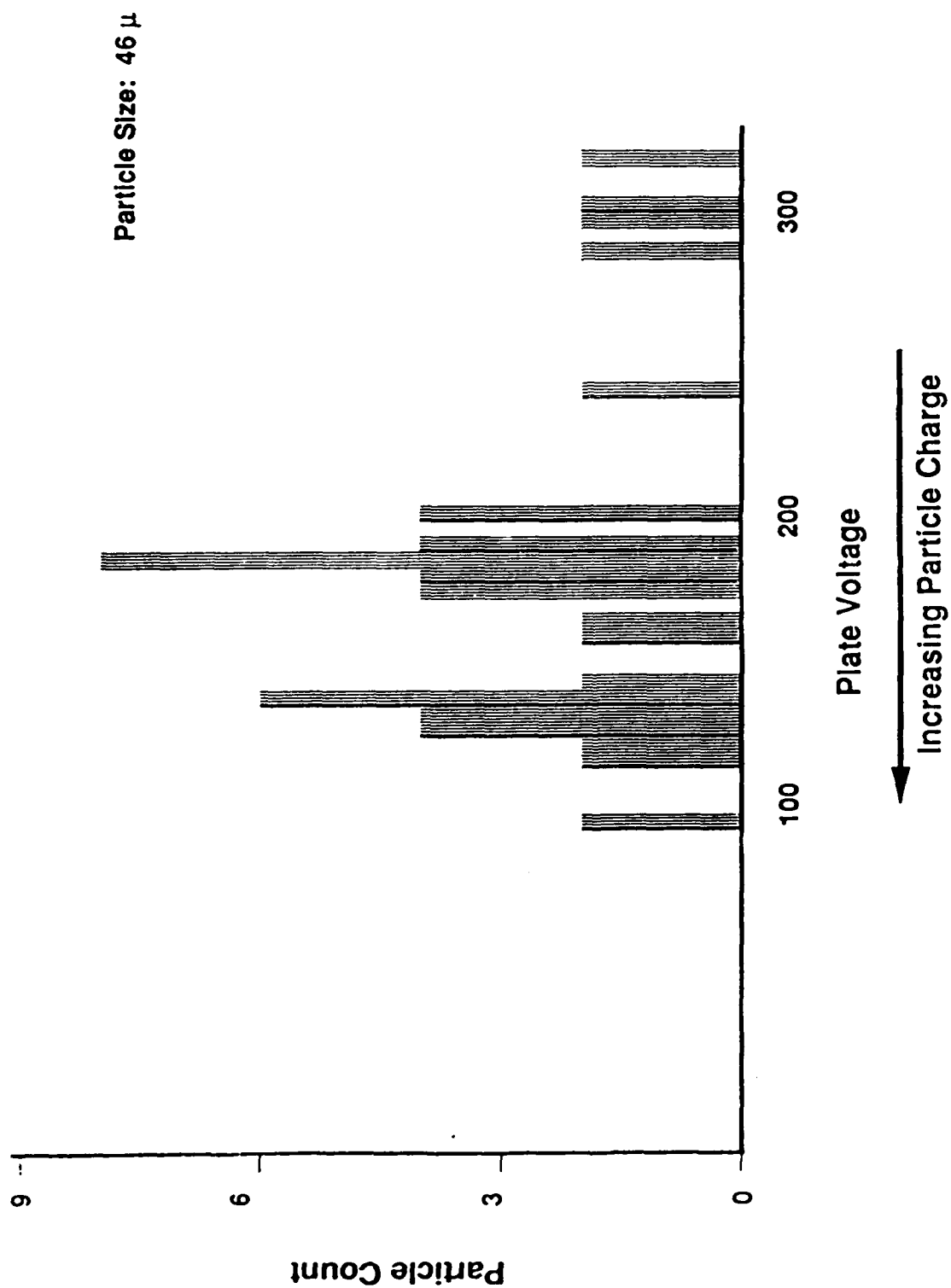


Figure 1 2

Charge Distribution for Copper. Corona Discharge Device was Off.
The Initial Electrostatic Balance Plate Voltage was 100 Volts.

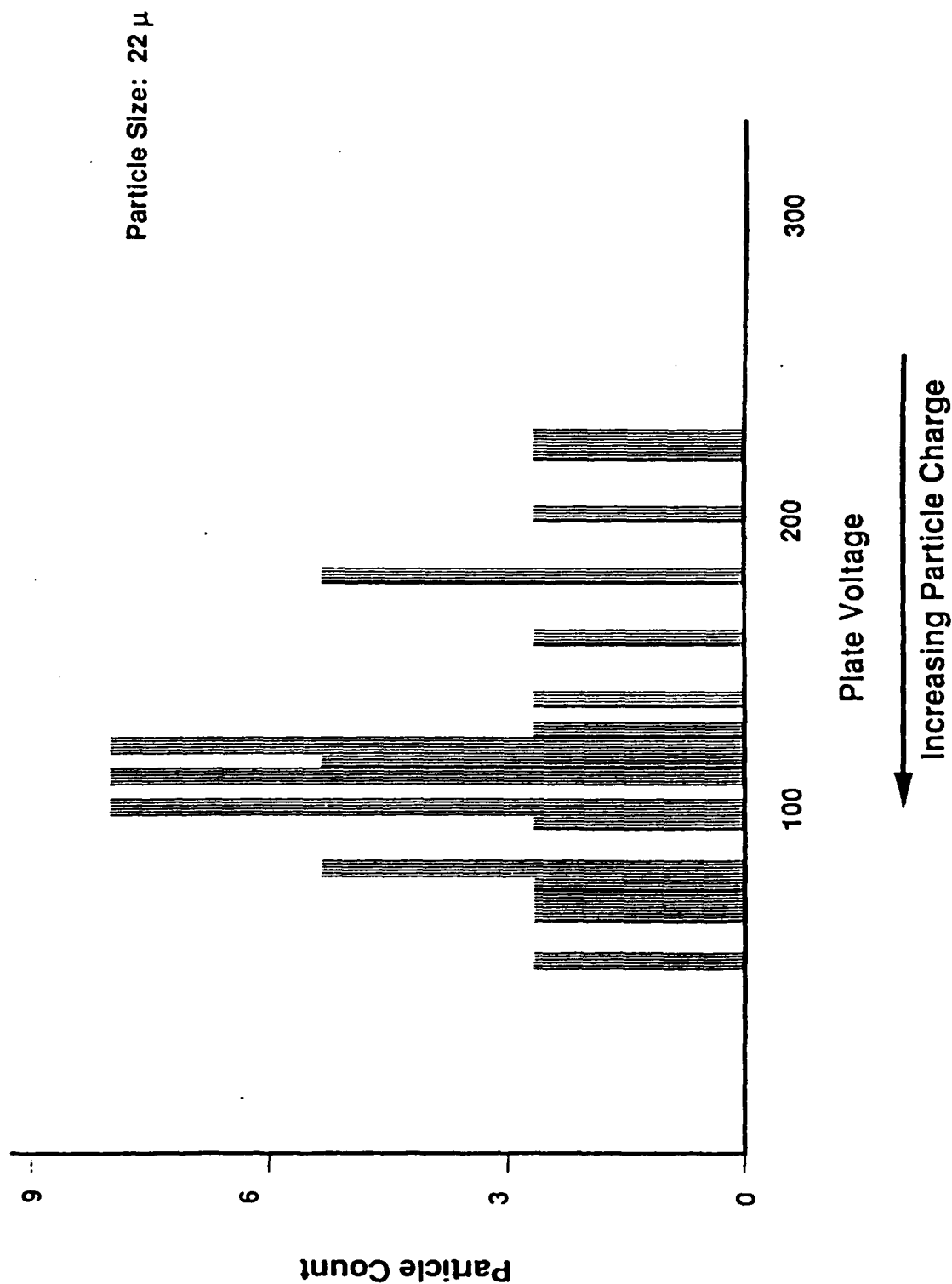


Figure 13

Charge Distribution for Iron. Corona Discharge Device was Off.
The Initial Electrostatic Balance Plate Voltage was 100 Volts.

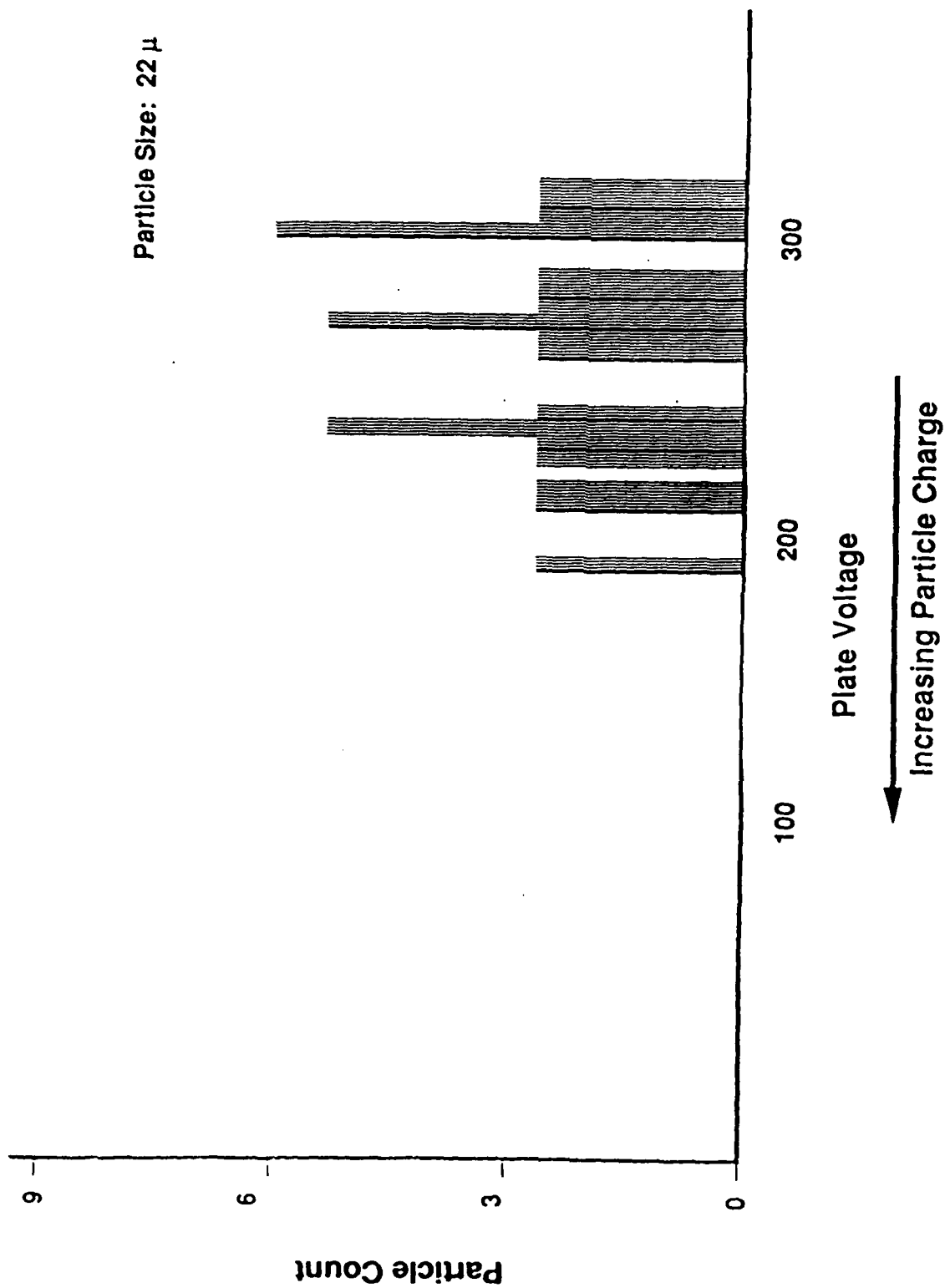


Figure 14

Charge Distribution for Lead. Corona Discharge Device was Off.
The Initial Electrostatic Balance Plate Voltage was 100 Volts.

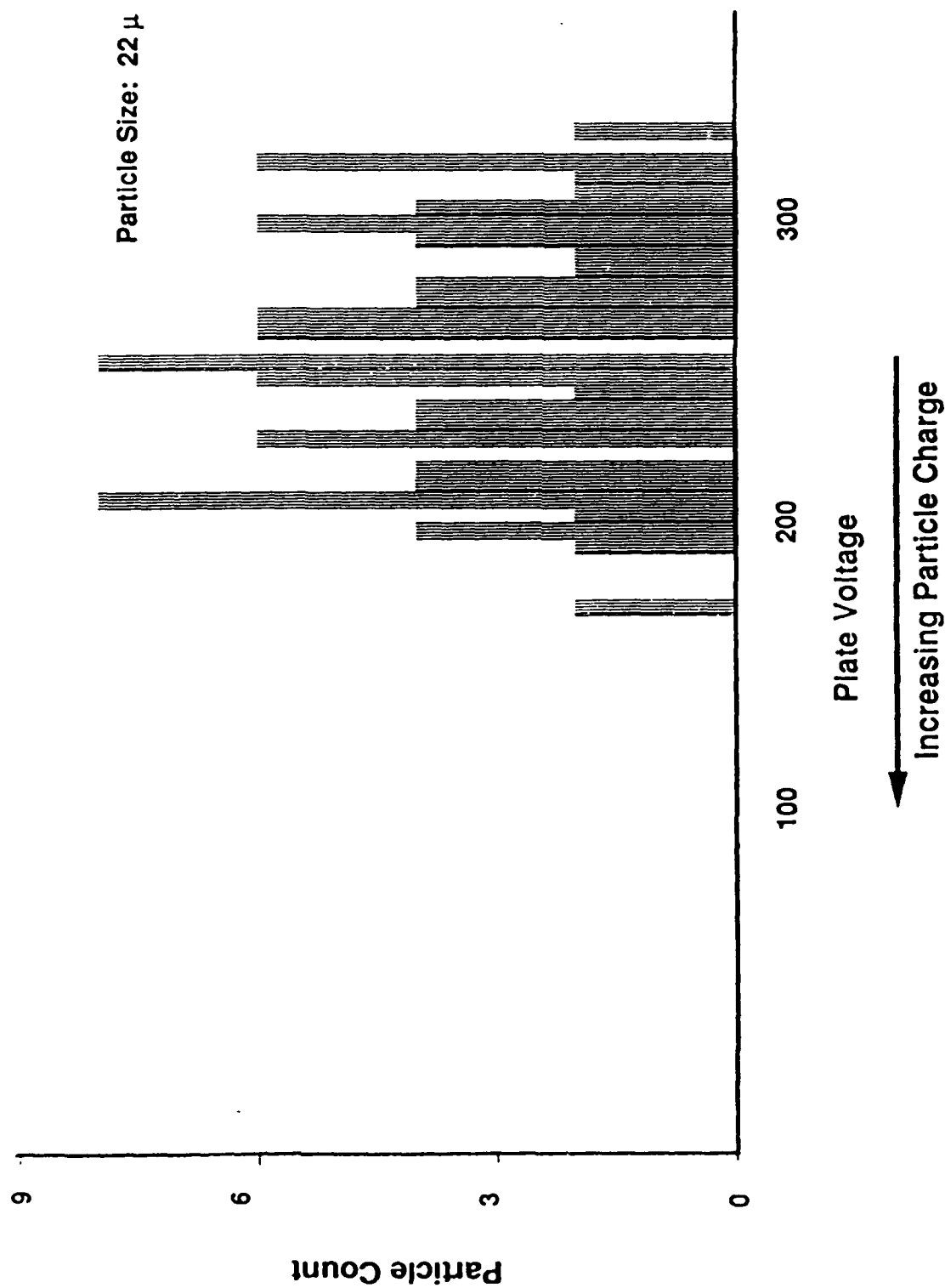


Figure 1-5

Charge Distribution for Magnesium. Corona Discharge Device was Off. The Initial Electrostatic Balance Plate Voltage was 100 Volts.

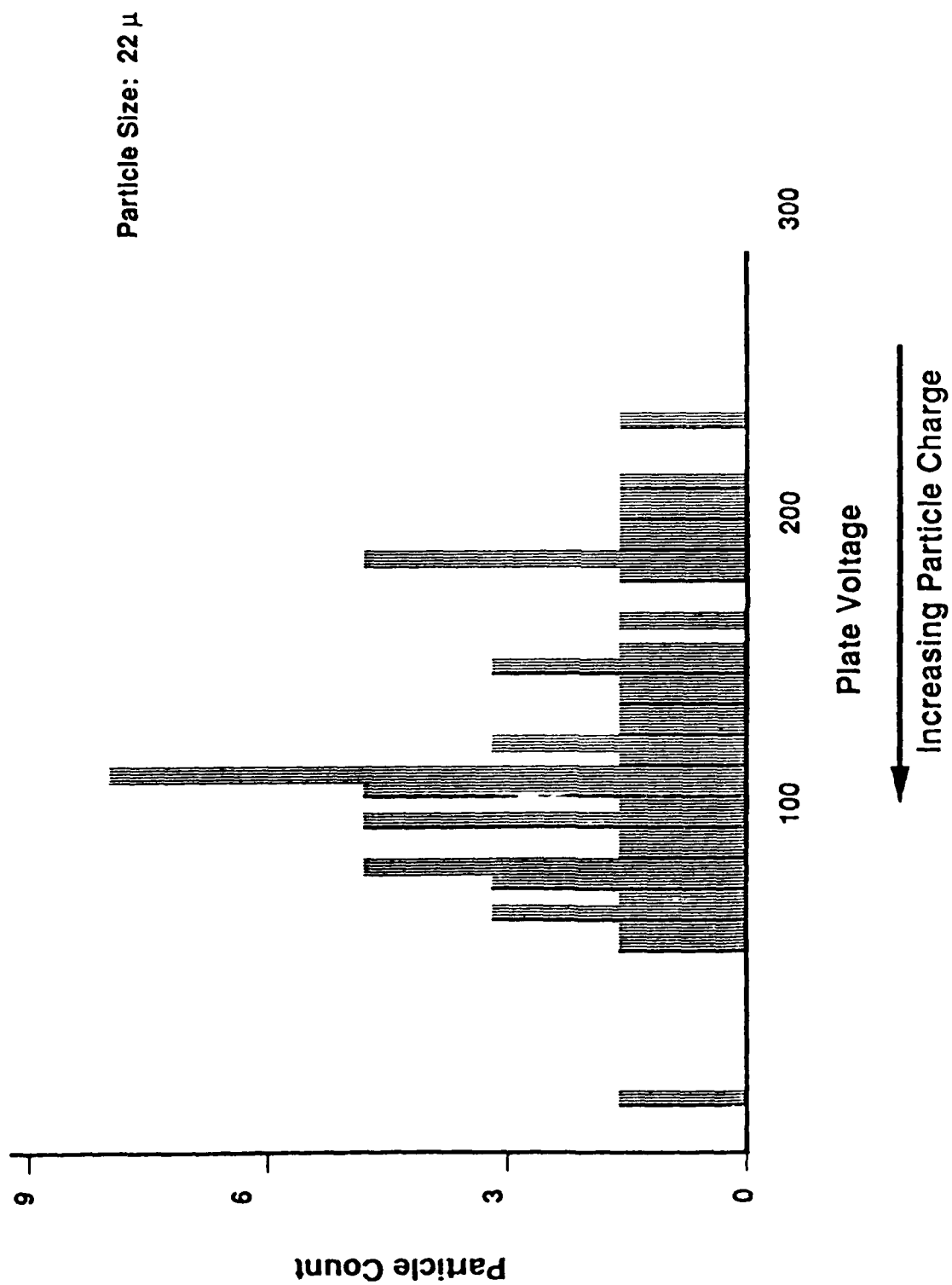


Figure 16
Charge Distribution for Glass Micro-Sphere. Corona Discharge Device was Off. The Initial Electrostatic Balance Plate Voltage was 100 Volts.

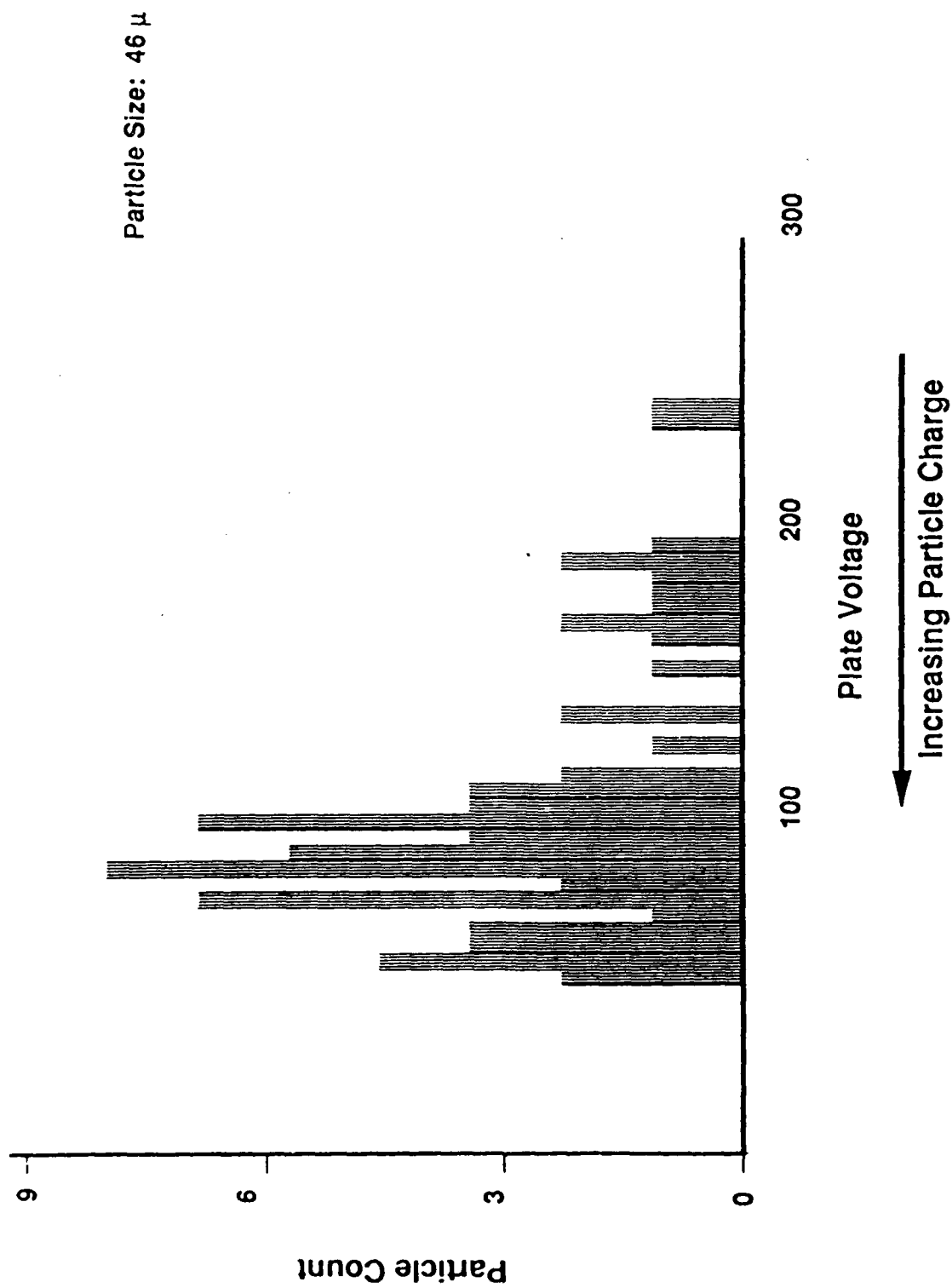


Figure 17

Charge Distribution for Graphite. Corona Discharge Device was Off. The Initial Electrostatic Balance Plate Voltage was 100 Volts.

	Al	Cu	Fe	Pb	Mg	Gr.	Gl.
Maximum Observed Particle Charge (Figures 11-17 and eq. 1) $\times 10^{-14}$ Coulombs	2.4	28.	4.5	2.1	3.0	15.	.65
Mean Of Observed Particle Charge Distribution (Figures 11-17 and eq. 1) $\times 10^{-14}$ Coulombs	.68	15.	2.1	1.5	2.1	6.4	.10
Theoretical Maximum Particle Charge (eq. 7) $\times 10^{-14}$ Coulombs	4.1	18.	4.1	4.1	18.	18.	4.1
Ratio Of Maximum Observed Particle Charge To Theoretical Particle Charge	.59	1.5	1.1	.51	.17	.83	.16
Ratio Of Mean Observed Particle Charge To Theoretical Particle Charge	.16	.83	.51	.37	.12	.36	.02

**Table 1 : Maximum Observed and Theoretical Particle Charge For
Al, Cu, Fe, Pb, Mg, Graphite and Glass, as Calculated From
Equations 1 and 7 and Figures 11-17.**

From Table 1 it is evident that the conductors and the graphite have higher characteristic charge and higher observed-to-theoretical ratios than does the glass dielectric, suggesting dielectrics may not be as good scavengers as non-dielectrics. A possible explanation may be shape effects. The dielectric glass particles were truly spherical whereas all the conductors were ellipsoidal with a wide range of aspect ratios.

4.3 Active Corona Discharge Particle Charging

Charge distributions have been measured for three materials: Al, Cu, and glass, after they pass through the corona discharge device. The distributions are shown in Figures 18-20. There is essentially no statistical difference between the active and passive (10 feet plastic tubing) particle charge distributions. There are two possible explanations for these results.

First, the amount of charge on the particles may be close to saturation. Using Equation 7, the maximum particle charge that can be attained theoretically in air (i.e., electric field of 1×10^4 volt/cm) was calculated and is shown in Table 1. The ratio of observed charge to theoretical charge is also shown. For the conductors, this ratio is very close to unity and in the case of copper, greater than 1, which implies that little additional charge could be imparted by the corona field.

A second possible reason for the absence of charging in the corona field is the short resident time in the corona. Equation 8 relates particle charge to resident time in the corona field. For the particle to attain a saturation charge, the residence time in the corona must be much greater than the particle charging time

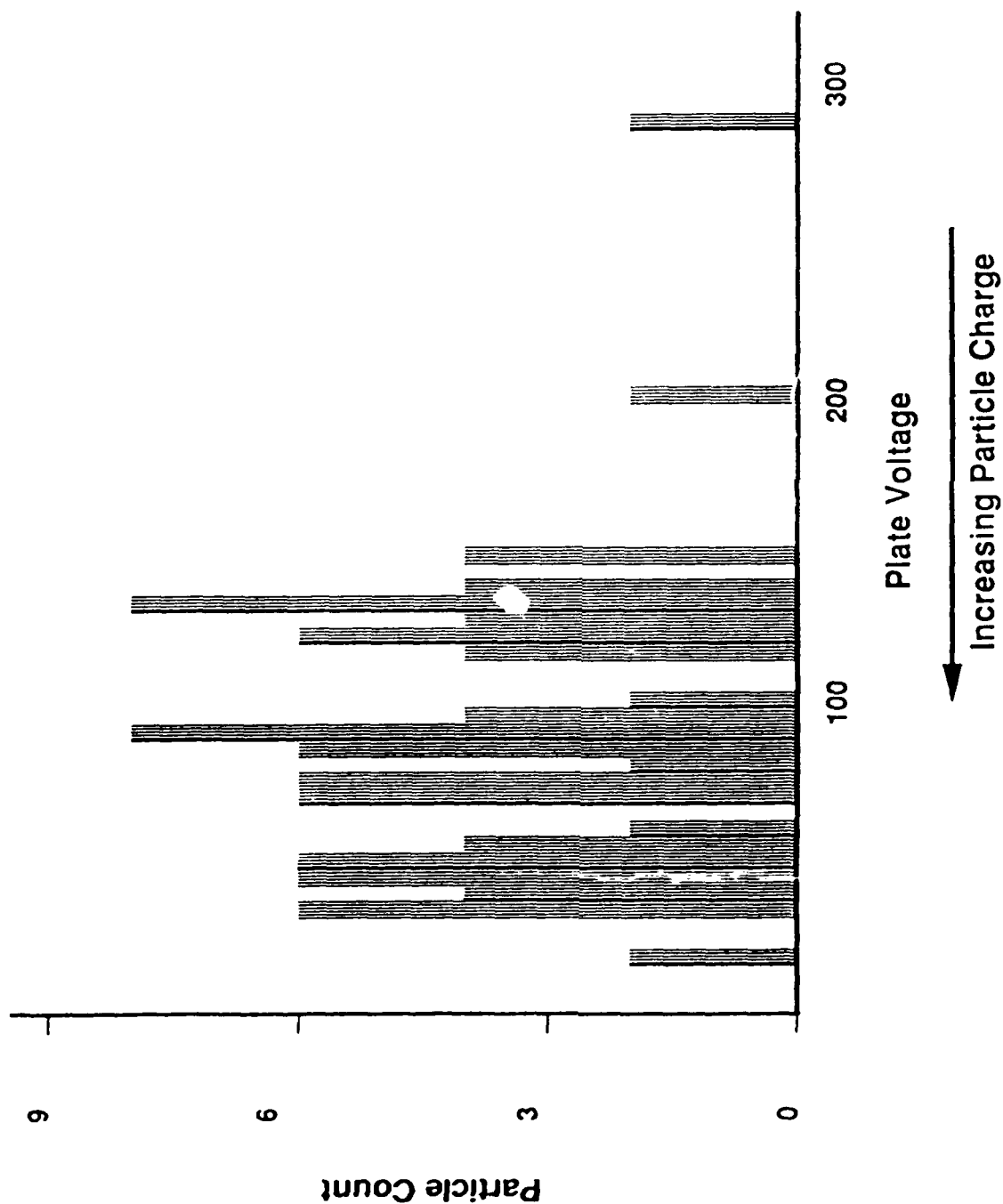


Figure 18
 Charge Distribution For Aluminum (particle size 22μ). The Corona Discharge Was Active And The Initial Electrostatic Balance Plate Was 100 Volts.

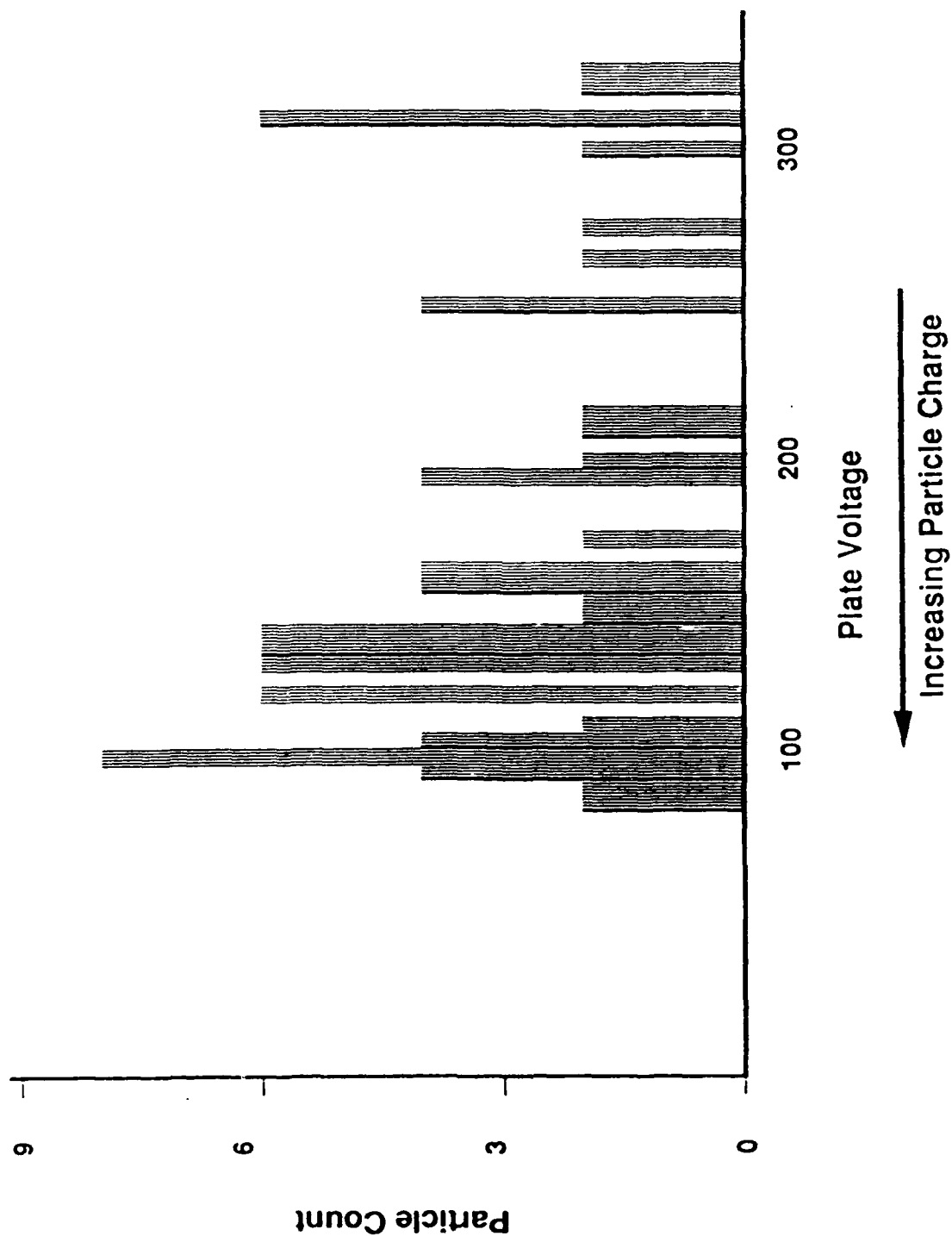


Figure 19
 Charge Distribution For Copper (particle size 46μ). The Corona Discharge Was Active And The Initial Electrostatic Balance Plate Was 100 Volts.

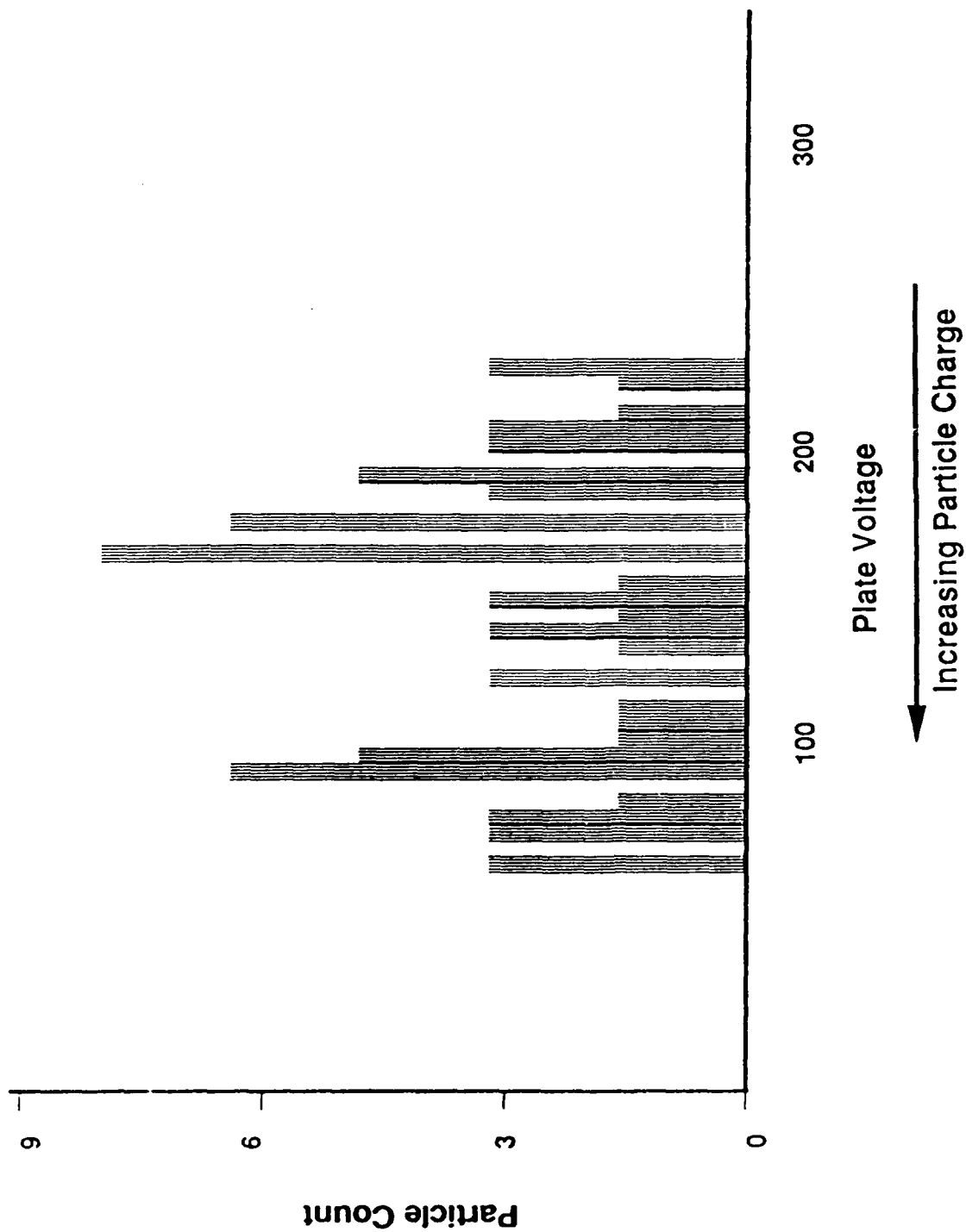


Figure 2-0
 Charge Distribution For Glass (particle size 22 μ). The Corona Discharge Was Active And The Initial Electrostatic Balance Plate Was 100 Volts.

constant, i.e., $t \gg \tau$. Reist has stated that for particles on the order of tens of microns, 90% charging is achieved after approximately 0.4 seconds. In the present experiment, residence times are considerably less than 0.4 seconds. The short charging times may explain the small differences observed between the active and passive charge distributions.

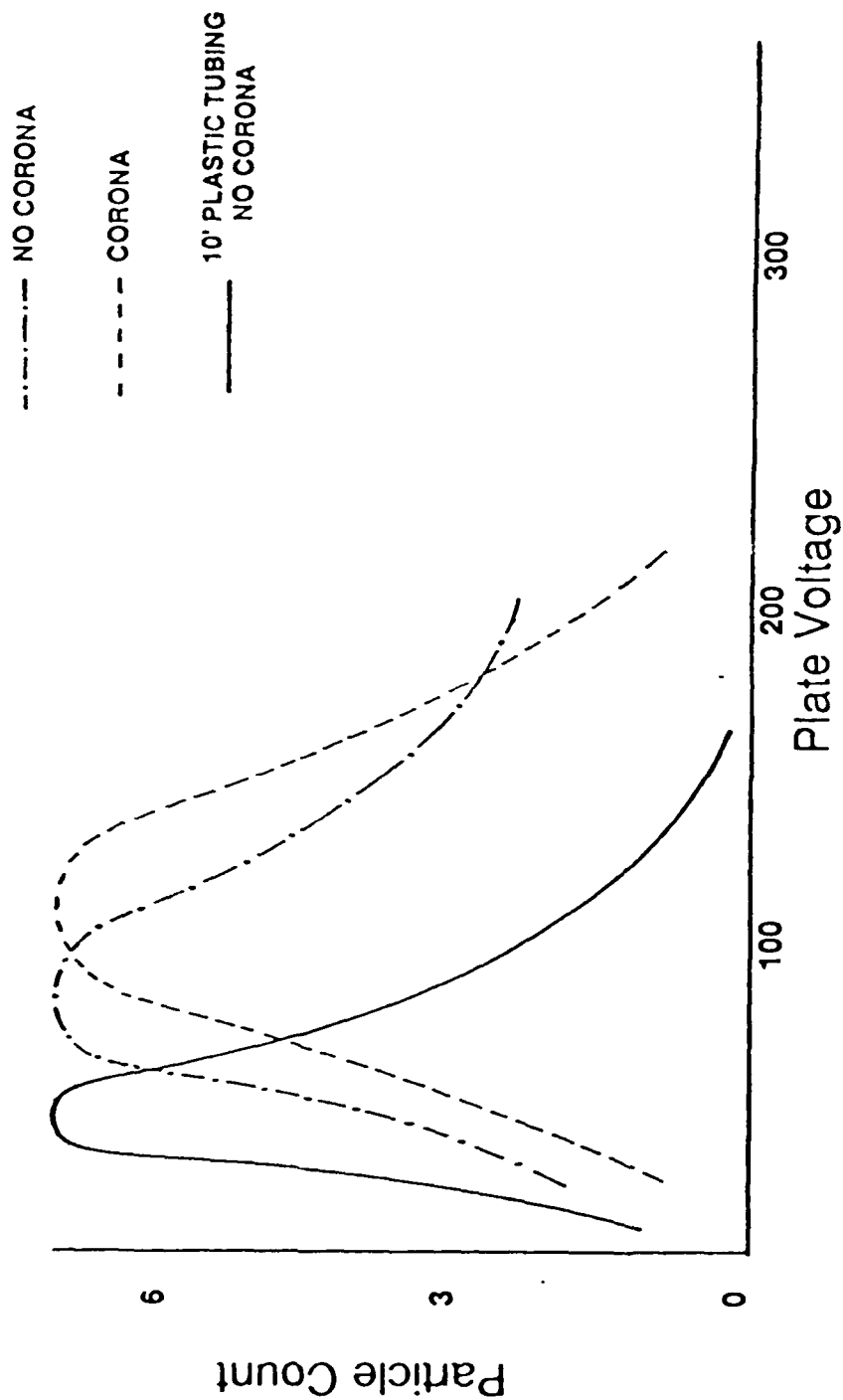
4.4 Triboelectric Particle Charging

Particle charging by a passive mechanism, triboelectrification was investigated. Aluminum was passed through a ten foot length of plastic tubing before it entered the balance. A comparison between this charging method and the corona (active and passive) is shown in Figure 21. There is a distinct shift in the particle charge distribution for the triboelectrically charged particles indicating an overall increase in scavenger charging.

The resultant increase in particle charging is noteworthy as it represents a low cost, low power, and potentially integrated directional disbursement method for deploying scavenging material. The exact mechanism for the triboelectric charging, whether the additional charge is from the tubing, the air, or both, is not well understood and should be examined in the Phase II program.

4.5 Terminal Velocity Experiments

Scavenger particle terminal velocity was determined by measuring the time required for a particle to freefall a distance of 1 mm. This measurement was made subsequent to the suspension of the particle in the electrostatic balance by removing the



Increasing Particle Charge

Effect Of Charging Method On Particle Charge (Aluminum, 22μ).
Initial Plate Voltage: 100 Volts.

Figure 21

voltage across the plates and measuring the time required for the particle to traverse a distance of 1 mm across a grid in the microscope field of view.

Terminal velocity measurements were performed using aluminum particles (20 microns in diameter) and glass microspheres (45 microns in diameter). It was observed that under our experimental conditions, and with such small particles, there was turbulence in the flow stream making our data inconclusive. In a future chamber design, horizontal electrostatic confinement may solve this problem.

5. CONCLUSIONS AND RECOMMENDATIONS

In the Phase I program "Clearing of Military Smokes and Aerosols", GEO-CENTERS, INC. has designed, fabricated, and employed an apparatus to evaluate characteristic particle charge distributions for candidate scavenger materials. Particle characteristic charge distributions were measured and charging mechanisms were evaluated. It was demonstrated that, (1) the particle saturation charge can be achieved with a rather simple transport system consisting of tygon tubing; and, (2) conductors attained charge more easily than dielectrics. Although no quantitative relationship between particle surface shape (assuming similar surface areas), and maximum particle charging was demonstrated, these results suggest that this is an important effect.

Charge distribution results indicate that several of the materials investigated may be suitable scavengers. A passive particle charging mechanism has been identified that promises to be low cost, low power, rugged, and can be integrated to act as a

directional deployment method. Having successfully demonstrated the feasibility of charging particles to maximum extent using a rather low power, low cost and rugged system, the following recommendations are offered.

1. Extend the charge measurements to large scavenger particles (1mm) concentrating on optimum materials identified in Phase I.
2. Evaluate efficiency of triboelectric charging method for large scavenger particles.
3. Design and construct prototype particle charging and dissemination system capable of operating with the materials identified in task 1.
4. Evaluate efficiency of the prototype charged scavenger system for the clearing of Military Smokes and Aerosols under the environmental conditions and operational constraints of an outdoor test site.

REFERENCES

1. Podzimek, Josef, "Investigation of a Complex Technique of Smoke Particle Deposition on Scavengers", (CRDEC-CR-87057, 1987), p.7.
2. Reist, Parker C., Introduction to Aerosol Science, MacMillan Publishing Company, New York, pp. 148-150.